

## LOW-AMPLITUDE STRESS WAVE MEASUREMENT IN SPLIT HOPKINSON BARS USING A VISCOELASTIC POLYMERIC BAR: ROLE OF PULSE SHAPING

Fíla T.<sup>1</sup>, Falta J.<sup>2</sup>

**Abstract:** *The Split Hopkinson Pressure Bar (SHPB) technique is widely used for high strain-rate characterization, but its application to low-impedance materials is limited by low signal amplitudes and poor signal-to-noise ratio in conventional metallic bars. Polymeric viscoelastic bars offer improved sensitivity but introduce wave dispersion, complicating signal interpretation. This study proposes a simplified approach combining a linear elastic aluminium input bar with a viscoelastic polyamide output bar and a wave separation technique based on simultaneous strain and velocity measurements at a single location. Instead of employing complex viscoelastic models, an effective linear elastic representation of the viscoelastic bar is calibrated using void tests. The results show that the approach is only valid when the frequency bandwidth of the stress wave is sufficiently reduced. Without pulse shaping (mechanical filtering), strong dispersion leads to significant discrepancies in measured signals. By introducing a soft copper pulse shaper, high-frequency components are suppressed, enabling accurate reconstruction of force and velocity using the simplified model. The method is successfully demonstrated on a very low-impedance material, where the polymeric bar provides significantly improved signal quality compared to a conventional metallic bar.*

**Keywords:** Split Hopkinson bar, Viscoelastic bar, Stress waves, Pulse shaping, Low impedance materials

### 1. Introduction

The Split Hopkinson Pressure Bar (SHPB) is a well-established method for determining material behavior at high strain rates due to its reliability and relative simplicity. However, it is limited for low-impedance materials (Bacon, 1998), where small deformation forces produce weak signals in conventional metallic bars, resulting in poor signal-to-noise ratios and reduced measurement accuracy. Polymeric viscoelastic bars with lower Young's modulus improve sensitivity (Bacon, 1998; Zhao and Gary, 1997), but introduce dispersion and attenuation, distorting stress waves. These effects are typically corrected using viscoelastic wave propagation models based on experimental transfer functions (Bacon, 1998) or constitutive models (Zhao and Gary, 1997; Bacon, 1999). Both approaches have drawbacks: experimental calibration may overfit, while constitutive modeling is complex and uncertain. Wave separation methods mitigate dispersion but require multiple measurement locations and extensive calibration (Zhao and Gary, 1997; Bussac et al., 2002; Lundberg and Henchoz, 1977; Casem et al., 2003).

Here, a simplified approach is proposed combining a linear elastic input bar with a viscoelastic output bar. Wave separation is performed using simultaneous strain and velocity measurements at a single location on each bar (Casem et al., 2003; Fíla et al., 2025). The viscoelastic bar is approximated as an effective linear elastic medium, calibrated via void tests. Reliable results are obtained when stress wave bandwidth is limited, achieved through pulse shaping to suppress high-frequency dispersion.

---

<sup>1</sup> Tomáš Fíla: Czech Technical University in Prague, Faculty of Transportation Sciences, Konviktská 20; 110 00, Prague; CZ, [fila@fd.cvut.cz](mailto:fila@fd.cvut.cz)

<sup>2</sup> Jan Falta: Czech Technical University in Prague, Faculty of Transportation Sciences, Konviktská 20; 110 00, Prague; CZ, [falta@fd.cvut.cz](mailto:falta@fd.cvut.cz)

## 2. Materials and Methods

### 2.1. Split Hopkinson Pressure Bar Setup

Experiments were conducted on a universal Split Hopkinson Bar (USHB) system in compression at Dyn-Lab, Faculty of Transportation Sciences, Czech Technical University. The setup targets low-impedance materials using a hybrid configuration with a metallic input bar and a viscoelastic polymeric output bar. The input bar was aluminium alloy EN-AW-7075 (3000 mm length, 30 mm diameter), while the output bar was polyamide PA6 (3070 mm length, 30 mm diameter). An aluminium striker bar (2700 mm length) generated the incident pulse and was accelerated by a gas gun with a 3000 mm barrel, enabling controlled impact velocities. Stress waves generated in the input bar propagated into the viscoelastic output bar, where dispersion and attenuation influenced their evolution.

### 2.2. Stress Wave and Velocity Measurements

Stress wave propagation was measured via simultaneous strain and particle velocity acquisition at a single location on each bar. Axial strain was recorded using HBM foil strain gauges, and particle velocity using a magnetic linear encoder (LM10, RLS, Slovenia). This enabled wave separation into forward- and backward-propagating components (Fíla et al., 2025). Signals were acquired at 1 MHz using a high-speed, low-noise system, providing sufficient temporal resolution for transient wave capture. Data were processed using the referenced wave separation algorithm to reconstruct stress wave evolution. Calibration of the viscoelastic output bar was performed using void tests, where input and output bars were in direct contact, allowing direct assessment of wave transmission and effective propagation parameters. Additional tests used low-density cork as a very low-impedance specimen to evaluate performance under realistic conditions, with two impact velocities to assess rate effects. The influence of pulse shaping on wave frequency content was investigated via void tests with and without a pulse shaper. The shaper, a  $\sim 1$  mm thick soft copper disk at the input bar interface, modified the incident pulse by attenuating high-frequency components. This reduced bandwidth is essential to limit Pochhammer–Chree dispersion in the viscoelastic bar, minimizing signal distortion and enabling the use of simplified wave propagation models.

### 2.3. Wave Correction Procedure

Correction of stress waves in the viscoelastic output bar was based on calibration from void tests. Signals from the aluminium input bar were first processed and time-shifted to the bar interface using linear elastic wave relations and known material properties, providing a reliable reference for force and particle velocity. Continuity conditions require equality of force and velocity across the interface, which was independently confirmed by high-speed imaging, showing no separation or slip. The polyamide bar response was then calibrated to match these reference signals.

An effective linear elastic model of the viscoelastic bar was introduced, with parameters - effective nominal wave speed and Young’s modulus - identified by fitting polyamide signals to the interface reference. Calibration was performed with and without pulse shaping to assess bandwidth effects on the linear approximation. Both strain- and velocity-based signals were used, and their consistency verified. The resulting effective parameters are summarized in Table 1.

*Tab. 1: Materials constants of linear elastic models*

	Aluminum alloy EN-AW-7075	Polyamide PA6
Dynamic Young’s modulus [MPa]	72000	3525
Wave propagation velocity [m/s]	5218	1670

## 3. Results

Void test results demonstrate the necessity of pulse shaping to control stress wave bandwidth. Comparison of force and velocity signals from the aluminium input bar and polyamide output bar shows that,

without pulse shaping, force remains relatively consistent, but velocity exhibits significant discrepancies (Fig. 1). This indicates strong dispersion in the viscoelastic bar, where broad frequency content and high-frequency components are affected by Pochhammer–Chree dispersion. Consequently, velocity signals in the polyamide bar deviate markedly from the aluminium reference, showing that a linear elastic approximation is insufficient and that accurate correction would require frequency-domain viscoelastic models with transfer functions.

With pulse shaping, high-frequency components are suppressed, reducing bandwidth and dispersion effects. Force and velocity signals from both bars then agree well (Fig. 2), validating the effective linear elastic approximation for sufficiently smooth, low-frequency waves. A key observation is the noise difference: the aluminium bar exhibits high noise due to its high stiffness and low strain amplitudes under low-force loading, reducing sensitivity. In contrast, the polyamide bar provides larger strains and a significantly improved signal-to-noise ratio, making it more suitable for low-impedance materials.

Performance is further demonstrated on low-density cork tested at two impact velocities. Force–displacement curves show that aluminium bar data are dominated by noise and unsuitable for force evaluation, though still usable for velocity and displacement. The calibrated polyamide bar yields smooth, consistent force signals (Fig. 3). Wave separation additionally enables analysis of multiple wave reflections, allowing evaluation over extended loading, including later deformation stages such as densification, especially at higher impact velocities.

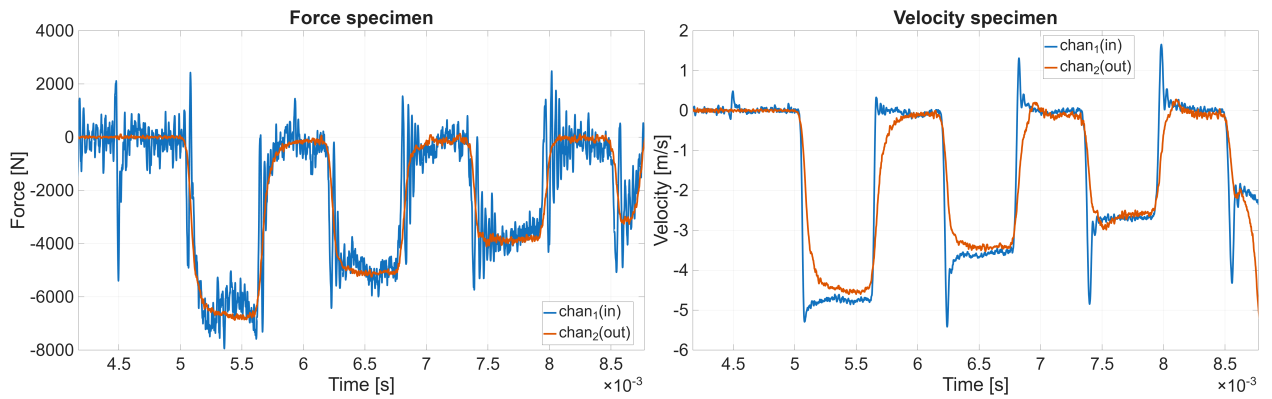


Fig. 1: Force-time (left) and velocity-time (right) diagrams showing differences of force and velocity data from input aluminum alloy bar (blue curve) and output polyamide bar (red curve) during a test without a pulse shaper.

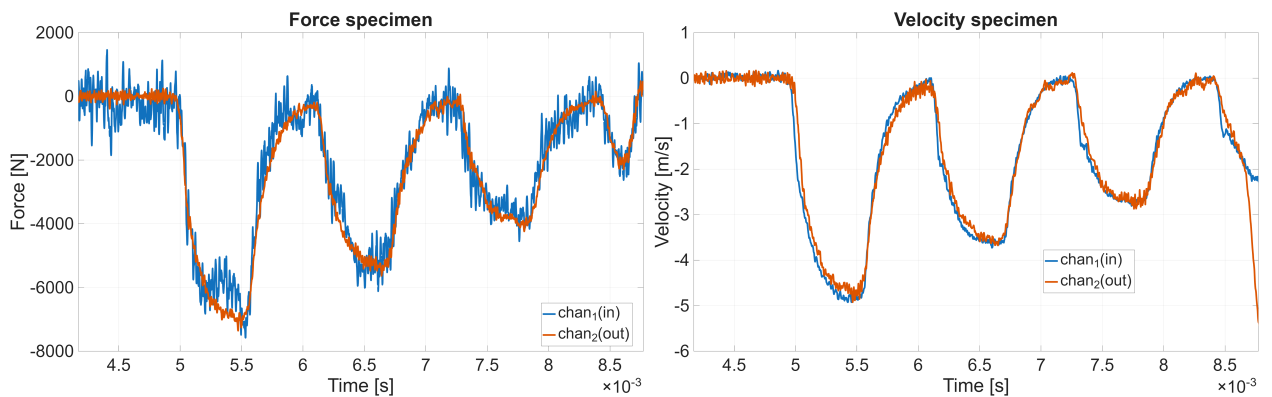


Fig. 2: Force-time (left) and velocity-time (right) diagrams showing consistency of force and velocity data from input aluminum alloy bar (blue curve) and output polyamide bar (red curve) during a test with a pulse shaper.

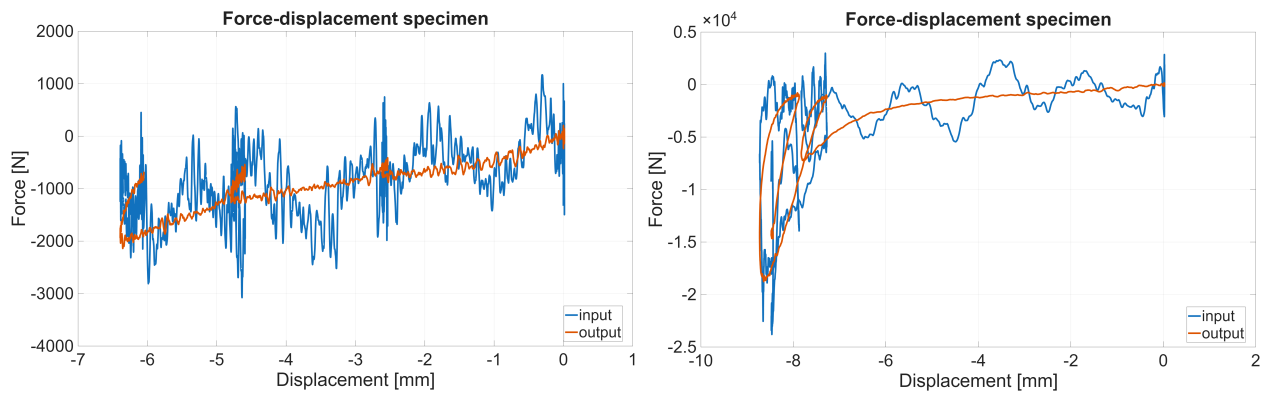


Fig. 3: Force-displacement diagram of soft cork specimen at a velocity of 5 m/s (left) and 15 m/s (right) showing extensive difference between noise in aluminum alloy bar (blue curve) and polyamide bar (red).

#### 4. Conclusions

A hybrid Split Hopkinson bar configuration combining a linear elastic aluminium input bar and a viscoelastic polyamide output bar was shown to enable reliable measurement of low-amplitude stress waves when combined with a wave separation technique and velocity–strain measurements. The study demonstrates that a simplified effective linear elastic model of the viscoelastic bar is only valid when the frequency bandwidth of the stress wave is reduced. Without pulse shaping, wave dispersion effects are too significant and require a full viscoelastic treatment. By introducing a soft copper pulse shaper, the frequency content is sufficiently limited, allowing accurate correction using the proposed approach.

#### Acknowledgments

The research was supported by the Czech Science Foundation (project Junior Star no. 22-18033M).

#### References

- Bacon, C. (1998) An experimental method for considering dispersion and attenuation in a viscoelastic Hopkinson bar. *Experimental Mechanics*, 38, 4, pp. 242–249.
- Bacon, C. (1999) Separation of waves propagating in an elastic or viscoelastic Hopkinson pressure bar with three-dimensional effects. *International Journal of Impact Engineering*, 22, 1, pp. 55–69.
- Bussac, M.-N., Collet, P., Gary, G., and Othman, R. (2002) An optimisation method for separating and rebuilding one-dimensional dispersive waves from multi-point measurements. Application to elastic or viscoelastic bars. *Journal of the Mechanics and Physics of Solids*, 50, 2, pp. 321–349.
- Casem, D., Fourney, W., and Chang, P. (2003) Wave separation in viscoelastic pressure bars using single-point measurements of strain and velocity. *Polymer Testing*, 22, 2, pp. 155–164.
- Fíla, T., Falta, J., and Dvořák, R. (2025) A simple wave separation method for split hopkinson bar experiments using linear encoders. *Results in Engineering*, 28, pp. 106980.
- Lundberg, B. and Henchoz, A. (1977) Analysis of elastic waves from two-point strain measurement: Strain, particle velocity, power transmission and related quantities can be determined at an arbitrary section of a cylindrical rod from measurement of strains at two different rod sections. *Experimental Mechanics*, 17, 6, pp. 213–218.
- Zhao, H. and Gary, G. (1997) A new method for the separation of waves. Application to the SHPB technique for an unlimited duration of measurement. *Journal of the Mechanics and Physics of Solids*, 45, 7, pp. 1185–1202.